

NUMERICAL METHODOLOGY OF PREDICTION OF THE RELIABILITY AND RESIDUAL LIFE OF WELDED PIPELINE ELEMENTS WITH CORROSION-EROSION DEFECTS

O.S. Milenin, O.A. Velykoivanenko, G.O. Rozyuka and N.I. Pivtorak

E.O. Paton Electric Welding Institute of the NAS of Ukraine

11 Kazymyr Malevych Str., 03150, Kyiv, Ukraine. E-mail: office@paton.kiev.ua

A set of procedures, mathematical models and tools for their finite-element realization were developed to solve typical practical tasks of expert analysis of the technological condition and residual safe operating life of welded elements of the main and technological pipelines with defects of corrosion-erosion metal loss detected during diagnostics. In order to lower the conservativeness of analysis, the interrelated processes of thermal deformation at assembly and repair welding, as well as initiation and propagation of subcritical damage of the defective structure material in the ductile mode in operation under complicated temperature-force conditions of external impact, were taken into account. Procedures of statistical analysis of fracture susceptibility of welded pipelines were developed on the base of Weibull and Monte-Carlo methods, and adequacy of the developed computational methods was confirmed. Peculiarities of the effect of welding on the reliability and serviceability of the main and technological pipelines with detected defects of corrosion-erosion metal loss were determined, in order to develop minimally conservative recommendations as to the possibility of safe operation of the pipelines. 18 Ref., 2 Tables, 12 Figures.

Keywords: pipeline, defect of corrosion-erosion metal loss, welded joint, limit state, reliability, fracture probability, ductile fracture

Determination of residual strength and serviceability of pipeline elements (PE) with detected defectiveness is a typical task in the complex of measures on analysis of the actual technical condition and ensuring reliable operation. In particular, for the main and technological pipelines in long-term service a typical phenomenon is accumulation of metal discontinuity defects, which lower their load-carrying capacity of the metal right up to emergency condition. The most wide-spread defects are surface thinning of the pipe wall. Their appearance is the result of structure interaction with the aggressive environment, or negative impact of the transported product. Assessment of admissibility of isolated defects of corrosion-erosion metal loss is regulated by a range of local and foreign normative documents, the generality of which requires significant conservatism. In particular, a typical engineering approach is an essential simplification or ignoring the features of the PE stress-strain state (SSS) in the area of assembly or repair welds in the case of presence of a wall thinning defect on its periphery. This is associated with the complexity of description of the processes of interaction of different types of stresses (residual and in the raiser zone) and appropriate development of subcritical fracture

of pipe material, that, in its turn determines the limit state of the defective PE.

In order to determine the limit state of welded structural elements under complex external impact and to solve the related applied problems, one of the modern tendencies in the world research practice is development of methods of numerical finite element prediction of spatial multiphysical processes, which determine initiation and development of material fracture. For the above problem of expert analysis of the reliability of welded PE with local metal losses, a goal was set in this study to develop a complex methodology of numerical prediction of residual SSS in the area of assembly (repair) welding, modeling the simultaneous development of stresses, strains, subcritical damage and to define the respective criteria of the limit state and reliability parameters.

Depending on design conditions of a specific PE operation, it was necessary to take into account different factors of impact on fracture susceptibility of a structure. As regards pipelines with revealed 3D defects of corrosion-erosion metal loss, the main mechanism of subcritical material damage is considered to be the ductile mechanism, which consists in initiation and development of material porosity of certain volume concentration f at plastic flow of metal under

the impact of external static or cyclic loading [1, 2]. Thus, numerical tracing of the stress-strain and damage state of a defective PE should take into account the features of external operational impact on the pipe material, in particular, on the kinetics of irreversible deformations that cause initiation and propagation of ductile fracture pores.

At determination of residual SSS in the area of assembly permanent joints, it is necessary to take into account both the impact of welding process parameters proper, and temperature dependencies of the main properties of the pipe material. For this purpose, numerical prediction of temperature field kinetics was performed in this study by solving a nonstationary equation of heat conduction. The thus obtained development of spatially distributed temperatures and the change of structural composition determine formation and subsequent redistribution of stresses and strains in structures that, in its turn, determines the features of limit state under operation conditions.

Modeling of the kinetics of SSS and subcritical damage was conducted within the finite-element definition of the boundary problem of nonstationary thermoplasticity and ductile fracture. So, the increment of deformation tensor in a specific finite element (FE) in welding and subsequent operation, allowing for presence of ductile fracture micropores was determined in keeping with the following expression [3]:

$$d\varepsilon_{ij} = d\varepsilon_{ij}^e + d\varepsilon_{ij}^p + d\varepsilon_{ij}^c + \delta_{ij} (d\varepsilon_T + df/3), \quad (1)$$

where $d\varepsilon_{ij}^e$, $d\varepsilon_{ij}^p$, $d\varepsilon_{ij}^c$, δ_{ij} , $d\varepsilon_T$, $\delta_{ij} \cdot df/3$ are the components of increments of tensor of strains due to elastic deformation mechanism, deformations of instantaneous plasticity, creep, kinetics of nonuniform temperature field and porosity, respectively, $(i, j) = \{r, b, z\}$ (Figure 1).

Increments of strain tensor were presented in the form of superposition of increment of the respective components [4, 5]:

$$\begin{aligned} \Delta\varepsilon_{ij} = & \left[\Psi + \Omega(\sigma_i^*, T) \Delta\tau \right] (\sigma_{ij} - \delta_{ij} \sigma) + \\ & + \delta_{ij} (K\sigma + \Delta\varepsilon_T + \Delta f/3) - \\ & - \left[\frac{1}{2G} + \Omega(\sigma_i^*, T) \Delta\tau \right] (\sigma_{ij} - \delta_{ij} \sigma)^* - (K\sigma)^*, \end{aligned} \quad (2)$$

where «*» symbol refers the respective variable to the previous tracing step; G is the shear modulus; $\Omega(\sigma_i, T) = A_c \exp\left(\frac{G_c}{T + 273}\right) \cdot \sigma_i^{n_c}$ is the creep function; n_c, A_c, G_c are the constants; Ψ — is the material state function that determines the condition of plastic flow

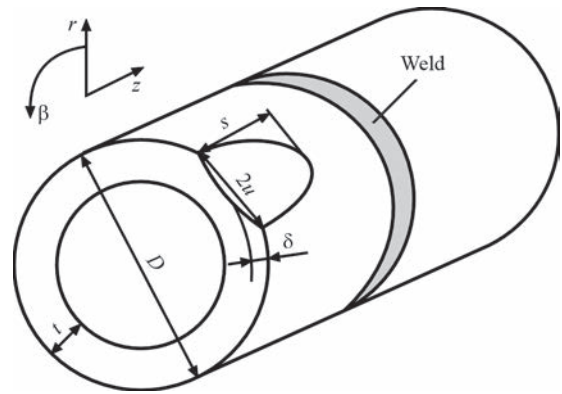


Figure 1. Scheme of a pipeline element with local defect of metal loss on the outer surface in a cylindrical system of coordinates

of metal in keeping with Gurson–Tvergaard–Needleman model [6]:

$$\begin{aligned} \Psi = & \frac{1}{2G} + \Omega(\sigma_i^*, T) \Delta\tau, \\ & \text{if } \sigma_i < \sigma_s = \sigma_T \times \\ & \times \sqrt{1 + (q_3 f')^2 - 2q_1 f' \cosh\left(q_2 \frac{3\sigma}{2\sigma_T}\right)}, \quad (3) \\ \Psi > & \frac{1}{2G} + \Omega(\sigma_i^*, T) \Delta\tau, \text{ if } \sigma_i = \sigma_s, \\ \sigma_i > & \sigma_s \text{ state is inadmissible.} \end{aligned}$$

Determination of function Ψ is performed by iteration at each step of numerical tracing. Additional nonlinearity by the subcritical damage at the change of the external force factor F is solved by the following iteration process by function Ψ_k [7]:

$$F = \begin{cases} F + dF, \text{ if } \int_0^1 K_1 \exp\left(K_2 \frac{\sigma}{\sigma_1}\right) d\varepsilon_1^p = \\ = \Psi_1 \leq \Psi_1^0 \approx 10^{-5}; \\ F, \text{ if } \Psi_1 > \Psi_1^0, \end{cases} \quad (4)$$

where F is the system of force loads that act on the structure; dF is the increment of force loads during numerical tracing.

Strain hardening of the metal influences the shape of Mises flow surface which, depending on the intensity of accumulated plastic deformations, is usually considered in the following form [8]:

$$\begin{aligned} \sigma_T = & \sigma_T^0 \left[1 + c_1 \ln\left(\frac{\dot{\varepsilon}^p}{\dot{\varepsilon}_0}\right) + c_2 \left\{ \ln\left(\frac{\dot{\varepsilon}^p}{\dot{\varepsilon}_0}\right) \right\}^2 \right] \times \\ & \times \left[1 + \left(\frac{\varepsilon^p}{\varepsilon_0}\right)^m \right] \end{aligned} \quad (5)$$

where $c_1 = 2.149 \cdot 10^{-3}$; $c_2 = 9.112 \cdot 10^{-2}$; $\varepsilon_0 = 1.540 \cdot 10^{-4}$, $m = 0.14$ are the constants; the dot over the variable denotes time differentiation.

If it is necessary to take into account the change of plastic deformation direction (for instance, at variable static loading, that causes alternating plastic deformation cycle), the following model of kinematic hardening of the material was used [9]:

$$\sqrt{\frac{3}{2}(\sigma_{ij} - \delta_{ij}\sigma - \bar{X})(\sigma_{ij} - \delta_{ij}\sigma - \bar{X})} - \sigma'_y(f') \left[1 + (\varepsilon^p/\varepsilon_0) \right]^M \leq 0, \quad (6)$$

where \bar{X} is the shear tensor; $\sigma'_y(f')$ is the current true yield limit of the damaged material, respectively (5); M, ε_0 are the material constants.

In order to predict ductile fracture initiation at plastic flow of the material of pipelines and pressure vessels from typical steels and alloys, modified Johnson–Cook criterion was used in nonisothermal cases, in keeping with which initial porosity of concentration f_0 develops in a certain metal volume, provided the following condition is fulfilled [10]

$$\chi_\varepsilon = \int \frac{d\varepsilon_i^p}{\varepsilon_c(T)} > 1, \quad (7)$$

where $d\varepsilon_i^p = \sqrt{2}/3 \cdot \sqrt{d\varepsilon_{ij}^p \cdot d\varepsilon_{ij}^p}$ is the intensity of increment of total plastic deformations (instantaneous plasticity and creep); $\varepsilon_c(T)$ is the critical value of plastic deformations.

Further increase of concentration of ductile fracture pores during plastic deformation of metal, in particular at static or cyclic loading in service, corresponds to modified Rice–Tracey law [11]. As the criterion of microscopic fracture initiation we proposed a numerical criterion of brittle-ductile fracture, namely satisfying one of the three conditions: plastic instability of porous material, taking into account its limited deformability by Mackenzie condition, critical development of pores and microcleavage S_K [12].

Definition of the limit state of a PE with a defect of local metal loss on the base of deterministic criteria cannot completely reflect the fracture susceptibility of a structure, as it considers fracture in the most critical point. In addition, indeterminateness of expert analysis that can be due to incompleteness of input data or inaccuracy of experimental measurements, requires respective increase of the conservativeness of the conclusions about PE technical condition. One of the alternative approaches that allow formally taking these factors into account, is application of integral statistical theories of strength. In particular, typical approaches to analysis of SSS of critical structures in terms of their fracture susceptibility, are based on Weibull’s statistical theory of strength [13]. It envis-

ages that damage initiation probability p is the function of the stressed state and it can be expressed using three-parameter Weibull distribution (σ -procedure). For the postulated problem of prediction of strength and operability of a steel or aluminium pipeline with revealed corrosion-erosion defects, it is formulated as follows:

$$p = 1 - \exp \left[- \int_S \left(\frac{\sigma_1 - A_\sigma}{B_\sigma} \right)^{\eta_\sigma} \frac{dS}{S_0} \right], (\sigma_1 > A_\sigma), \quad (8)$$

where σ_1 is the principal stress field; S is the pipe cross-sectional area; S_0 is the scale factor constant; $A_\sigma, B_\sigma, \eta_\sigma$ are the Weibull parameters.

Applicability of σ -procedure (8) is limited by the nature of subcritical damage of the material being considered, namely: if the structure does not lose its operability at plastic flow of metal up to reaching the limit state, the failure probability will be almost unchanged, accordingly, due to slight changes of stresses, whereas fracture probability will become higher. For instance, it is known that sufficient accumulation of creep deformations in the pipes at high-temperature operation leads to initiation and accumulation of subcritical porosity. However, no respective increase of stresses is observed here. Moreover, relaxation of stresses of a certain kind is observed (for instance, residual stresses in the welding zone). Thus, it can be concluded that models of (8) type are suitable for structures, the limit state of which is determined by brittle or ductile-brittle mechanisms of macrofracture (materials, embrittled as a result of radiation exposure or hydrogen saturation, etc.).

As the limit state of a pipeline with the detected metal loss depends mainly on ductile macrofracture (particularly, for ductile metals or in high-temperature operation), an alternative to (8) are Weibull models for probability assessment based on analysis of the structure deformed state (ε -procedure) in the following form [14]:

$$p = 1 - \exp \left[- \int_S \left(\frac{\varepsilon_i - A_\varepsilon}{B_\varepsilon} \right)^{\eta_\varepsilon} \frac{dS}{S_0} \right], (\varepsilon_i > A_\varepsilon), \quad (9)$$

where ε_i is the deformation intensity, derived at finite element analysis; $A_\varepsilon, B_\varepsilon, \eta_\varepsilon$ are the Weibull parameters.

In particular, for pipes from typical steels a series of numerical studies of the limit state, depending on the material properties and size of the semi-elliptical surface defect was performed (initial data for computations are as follows: $D \times t = 1420 \times 20$ mm, $E = 210$ GPa, $\nu = 0.3$, $\sigma_y = 300\text{--}600$ MPa, $f_0 = 0.01$, $S_K = 1000$ MPa, $\varepsilon_c = 0.01$). Solving the inverse problem showed that the dependencies of the conservative val-

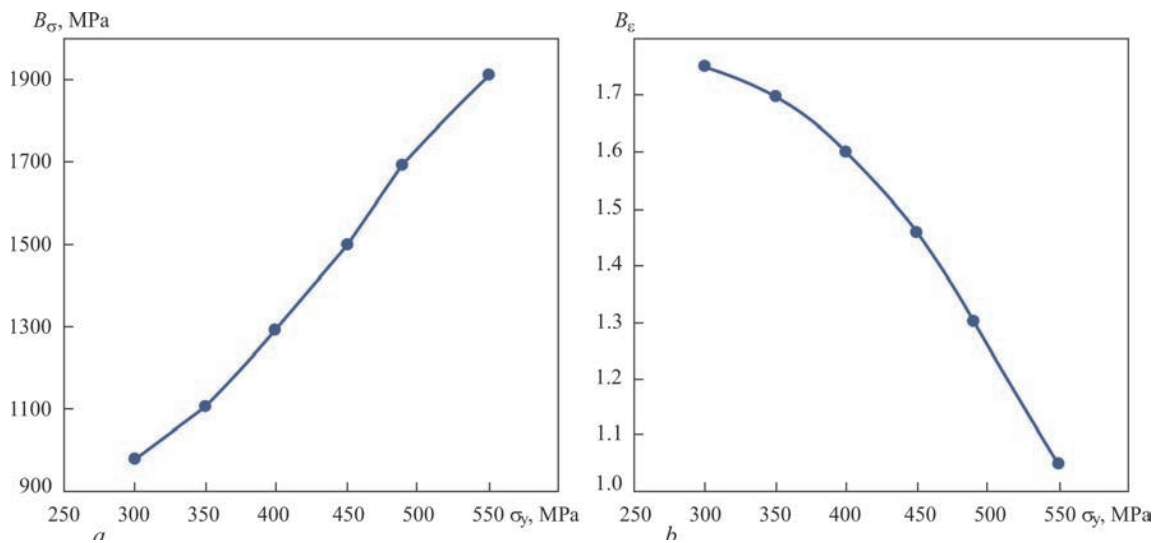


Figure 2. Dependencies of a conservative value of Weibull parameter B_σ (a) and B_ϵ (b) on yield limit σ_y of defective PE material (steel)

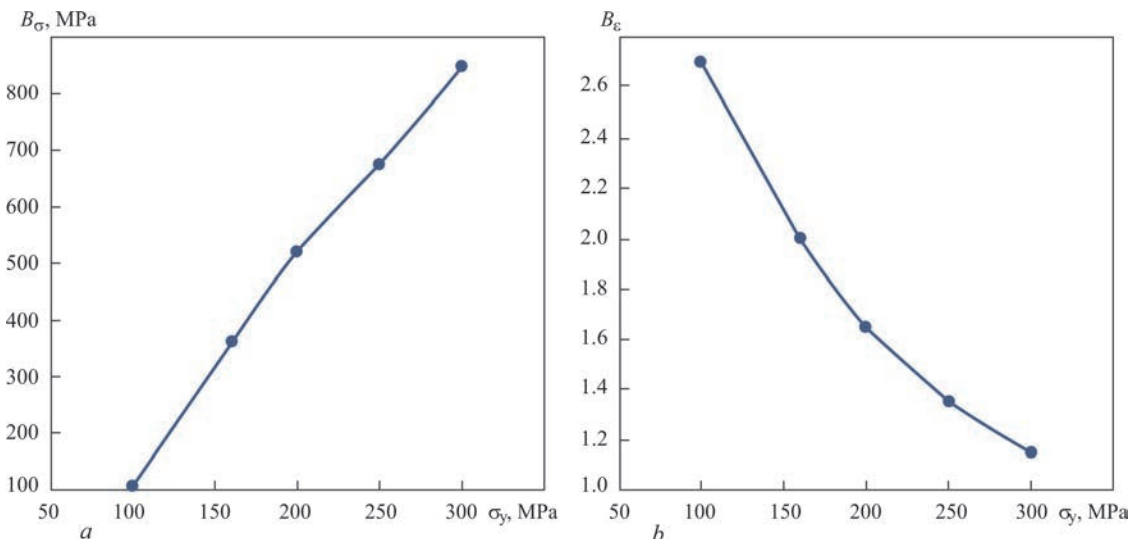


Figure 3. Dependencies of conservative value of Weibull parameter B_σ (a) and B_ϵ (b) on yield limit σ_y of defective PE material (aluminium alloys)

ues of Weibull B_σ and B_ϵ parameters on the yield limit σ_y of pipe steel are quasilinear (Figure 2) and only slightly depend on the size of the defect (range of the considered defect sizes in keeping with Figure 1 — $\delta = 3\text{--}17$ mm, $2s = 20\text{--}200$ mm; $2u = 20\text{--}200$ mm). Similar results were obtained for aluminium alloys of different strength (Figure 3).

In order to determine the effect of the scale factor, which is taken into account in the methodology of probabilistic integral analysis of stresses and strains (8)–(9) using S_0 parameter, statistic testing for uniaxial tension of 165×20 mm samples of different thickness (6 and 10 mm) from aluminium alloy AMg6 was conducted. Thinner samples were made from the same plate 10 mm thick by grinding off; permanent butt joint was produced by arc welding. As shown in Figure 4, 10 mm samples have consistently lower level of limit stresses, and fracture susceptibility is described by three-parameter Weibull function ($A_\sigma = 240$ MPa;

$B_\sigma = 250$ MPa; $\eta_\sigma = 4$), here S_0 corresponds to a value of 0.25 mm^2 for both the cases). This confirms prior conclusions that Weibull parameters in (8)–(9) are the

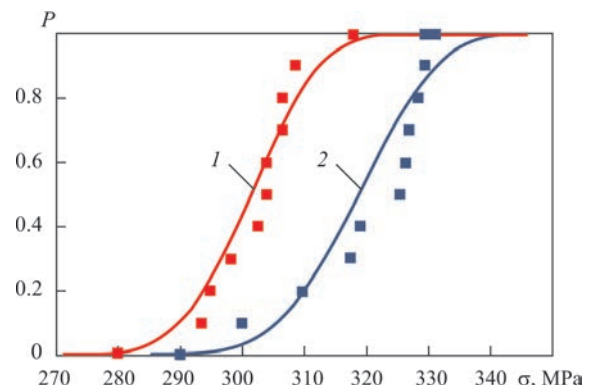


Figure 4. Determination of the impact of the scale factor (sample thickness) on fracture probability of welded samples from AMg6 aluminium alloy in keeping with theoretical calculation (solid line) and by the statistical laboratory testing (■): 1 — 10 mm thick samples, 2 — 6

material functions, and integration by the cross-section adequately takes the scale factor into account.

For the case of high-temperature operation of pipelines with detected defects of metal loss (for instance, erosion), fracture probability can be assessed using only the ε -procedure, taking into account the kinetics of creep deformation accumulation. As the material properties and its deformation susceptibility by the creep mechanism depend on temperature, temperature dependence of Weibull coefficients is to be expected. So, for typical steels 15Kh2NMFA and 10GN2MFA, which are widely used for manufacture of bodies and technological pipelines of NPP and TPP, the regularities of limit state formation under the conditions of simultaneous action of internal pressure and high temperature were studied in the case of an element of technological pipeline with a semi-elliptical defect of wall thinning; PE $D \times t = 300 \times 15$ mm. Coefficients of creep functions are as follows: 15Kh2NMFA — $n_c = 5.0$; $G_c = -101069$ °C; $A_c = \exp(69,40)$; 10GN2MFA — $n_c = 4.2$; $G_c = -61955$ °C; $A_c = \exp(34, 78)$ [15].

Derived by finite-element computation, distribution of deformations in the wall of a pipeline with a semi-elliptical defect of local thinning allowed solving the inverse problem of the limit state. This allowed determination of functional dependencies of B_ε parameter on material type and operating temperature. As shown in Figure 5, for 15Kh2NMFA and 10G2MFA steels temperature dependencies of B_ε are quasilinear for the selected temperature range and correspond to the range of values from 5.9 to 7.0. Here, the change of defect size only slightly affects the values of Weibull parameters.

It is known that the statistical theories of computation are based on the assumption of availability of indeterminateness of certain input data or physical processes. Statistical Weibull's theory of strength deals with macroscopic characteristics of the state

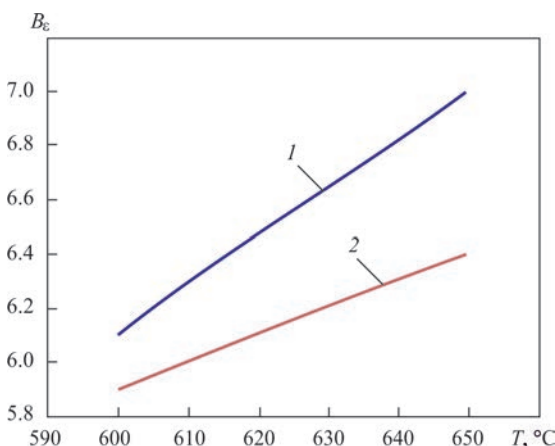


Figure 5. Dependencies of Weibull parameter B_ε of 10GN2MFA (1) and 15Kh2NMFA (2) steels on temperature

of material (stresses, strains) as characteristics of its microfracture susceptibility by the respective statistical description. Another typical factor of indeterminateness at analysis of the technical condition of structures in long-term service is the natural spatial scatter of material properties. Formal description of this phenomenon was performed using an algorithm based on Monte-Carlo method [16], within which it is assumed that pipeline fracture probability p at certain internal pressure P is determined by the frequency of achieving the limit state within a representative sample of equally possible combinations of pipe material properties, i.e.:

$$p(P) = N_p/N_r, \quad (10)$$

where N_p is the number of tests, at which the structure reached the limit state, at pressures lower than or equal to P , N_r is the total number of tests within the representative sample.

For formal description of spatial nonuniformity of such material properties as yield limit and Young's modulus, it is common to use the normal distribution, i.e. the probability density of X characteristic (assume a concrete value $X_{ijk}(i, j, k = r, \beta, z)$) can be presented in the following form:

$$\frac{\partial p}{\partial X_{ijk}} = \frac{1}{\beta_X \sqrt{2\pi}} \cdot \exp \left[-\frac{(X_{ijk} - \alpha_X)^2}{2\beta_X^2} \right], \quad (11)$$

$i, j, k = r, \beta, z,$

where α_X, β_X are the coefficients of normal distribution for X characteristic.

As regards different parameters of material fracture resistance, the Weibull distribution law is often used. Therefore, in the considered problem certain value Y in a point with coordinates (i, j, k) takes a specific value Y_{ijk} in keeping with the following relationship:

$$Y_{ijk} = [-\ln(1 - RND)]^{\frac{1}{\eta_Y}} (B_Y - A_Y) + A_Y, \quad (12)$$

$(i, j, k = r, \beta, z),$

where A_Y, B_Y, η_Y are the Weibull coefficients for Y characteristic; RND is an arbitrary number from the following range [0;1].

Validation procedure of the developed models for determination of limit state of PE with a wall thinning defect consists in comparison of limit pressure P_{max} , obtained within the numerical study, with the available experimental data [17] on failure pressure P_{exp} that are extensively used, in particular, in development of normative documents. For steel pipes of different strength classes calculations allowed precising the input parameters of the models and confirming the applicability of the developed approaches for PE of

Table 1. Comparison of the results of numerical computations of limit pressure P_{max} in defective pipeline elements with the results of experimental testing P_{exp} from international data bases (steel pipes of different strength classes) [17]

t , mm	D , mm	δ , mm	$2s$, mm	$2u$, mm	σ_y , MPa	Strength class	P_{exp} , MPa	P_{max} , MPa	Error, %
4.83	275	2.11	157.5	43.1	350.6	X42	12.62	13.80	9.35
5.00	274	2.16	124.5	43.1	350.6	X42	13.35	14.15	5.99
4.93	274	1.60	45.7	43.0	350.6	X42	14.99	16.40	9.41
4.88	273	2.18	101.6	42.9	350.6	X42	15.18	14.15	6.79
8.64	324	0.00	0.0	0.0	356.4	X46	24.44	25.15	2.91
8.64	324	0.00	0.0	0.0	356.4	X46	24.52	25.15	2.57
8.53	324	0.00	0.0	0.0	356.4	X46	25.01	25.15	0.56
8.51	324	0.00	0.0	0.0	356.4	X46	25.06	25.15	0.36
9.37	864	4.62	91.4	135.7	356.4	X46	9.17	8.35	8.94
9.47	864	3.00	185.4	135.7	356.4	X46	10.56	11.20	6.06
8.43	324	0.00	0.00	0.00	356.4	X46	23.27	25.15	8.08
8.74	324	0.00	0.00	0.00	356.4	X46	23.92	25.25	5.56
8.61	324	3.30	144.8	50.8	356.4	X46	23.93	22.60	5.56
8.64	323	2.16	63.5	50.8	356.4	X46	24.37	26.50	8.74
8.64	323	2.69	61.0	50.8	356.4	X46	25.23	25.20	0.12
5.26	273	1.73	139.7	42.9	402.5	X52	18.06	17.75	1.72
5.74	507	3.02	132.1	79.6	462.3	X55	10.73	10.25	4.47
17.50	762	8.75	200.0	50.0	464.5	X65	9.17	8.35	8.94
17.50	762	8.75	200.0	100.0	464.5	X65	10.56	11.20	6.06
17.50	762	4.38	200.0	50.0	464.5	X65	10.73	10.25	4.47

different typesizes, and also confirming the satisfactory accuracy of the developed procedures (Table 1).

As regards aluminium PE with local geometric anomalies of corrosion-erosion type, validation was also conducted by comparing the results of numerical prediction of the limit pressure in cylindrical samples from AA 6082 alloy with the data base of laboratory tests (Table 2) [18]. As shown by the results of comparison of the computational and experimental data, the error of numerical prediction of limit pressure is not more than 10 % that is sufficient for the majority of practical tasks.

Proceeding from the developed approaches, we studied the effect of assembly welding on the limit state of PE with local metal loss in typical cases of defective sections of the main and technological pipelines. We considered a steel element of the main pipeline ($D = 1420$ mm, $t = 20$ mm) with an isolated defect of local wall thinning of a semi-elliptical shape on the pipe outer surface ($2s \times 2u \times \delta = 20 \times 20 \times 5$ mm).

Presence of a circular weld leads to formation of a residual SSS in the assembly weld area and a change in the susceptibility to ductile fracture, as a result of presence of stress stiffness gradient $r_{st} = \sigma/\sigma_i$ (Figure 6). It should be noted that the stiffness of the structure stressed state is one of the factors that determine fracture resistance under the conditions of developed plastic flow of metal under the impact of external loading. Here, the strongest impact of local inhomogeneity of r_{st} in the area of the weld is observed at the first stages of plastic flow of PE metal under the impact of internal pressure, as a significant development of plastic deformation causes a certain homogenizing of the stressed state.

Thus, in case of presence in the area of a circular assembly weld of a local geometric anomaly in the form of surface metal loss, two sites of intensive development of subcritical metal damage at increase of internal pressure can be singled out: weld and HAZ with higher stiffness of the stressed state and geo-

Table 2. Comparison of the results of numerical computations of limit pressure in defective aluminium pipeline elements with the data of laboratory tests [18]

t , mm	D , mm	δ , mm	$2s$, mm	$2u$, mm	P_{exp} , MPa	P_{max} , MPa	Error, %
3.1750	145.542	1.6002	38.1508	9.525	10.5494	10.5	0.47
3.2512	145.694	1.6764	38.0492	38.0492	13.1695	11.9	9.64
2.8448	145.898	0.508	40.2336	10.1092	14.8243	14.5	2.19
2.8448	142.850	2.0066	38.2016	10.0076	7.23975	7.30	0.83
3.1496	137.871	2.413	12.1412	3.9878	14.4795	13.2	8.84
3.1242	137.820	2.540	6.1214	9.652	15.6861	16.6	5.83
3.1242	137.820	2.2606	59.6392	10.2616	6.55025	6.50	0.77
3.1496	137.871	2.3876	12.319	363.499	8.9635	9.40	4.87
6.2992	145.694	5.3594	53.4924	9.8298	11.7215	11.6	1.04
6.2484	145.593	4.699	13.7668	9.779	22.7535	24.1	5.92

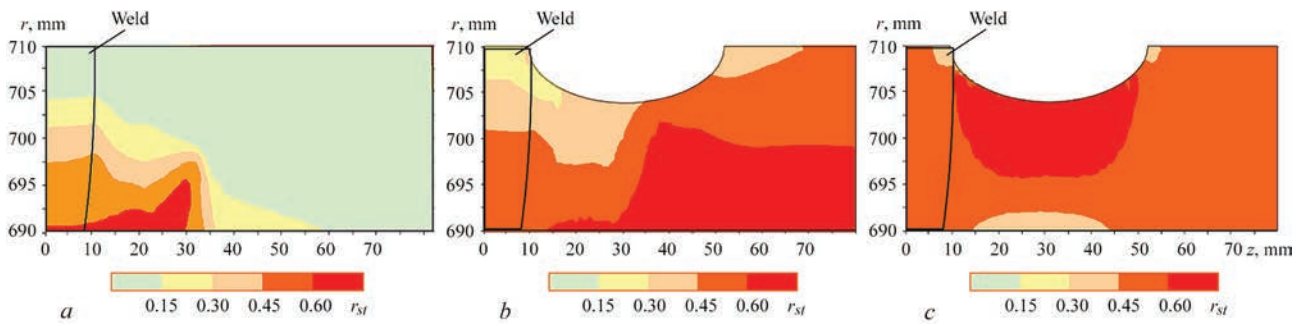


Figure 6. Distribution of stress stiffness r_{st} in the pipeline cross-section ($D \times t = 1420 \times 20$ mm, X65) with external corrosion defect ($2s \times 2u \times \delta = 40 \times 20 \times 5$ mm) in the circular weld area at internal pressure P : *a* — after welding; *b* — 7.5 MPa; *c* — at limit pressure of 22.8 MPa

metrical stress raiser proper (Figure 7). As a close location (smaller than the defect length) of the weld and metal loss, a common field of subcritical damage forms between them that has a negative impact on the

pipeline load-carrying capacity, as it is the site of potential initiation of a macrodefect.

In case of PE high-temperature operation, presence of a local stress raiser in the form of surface

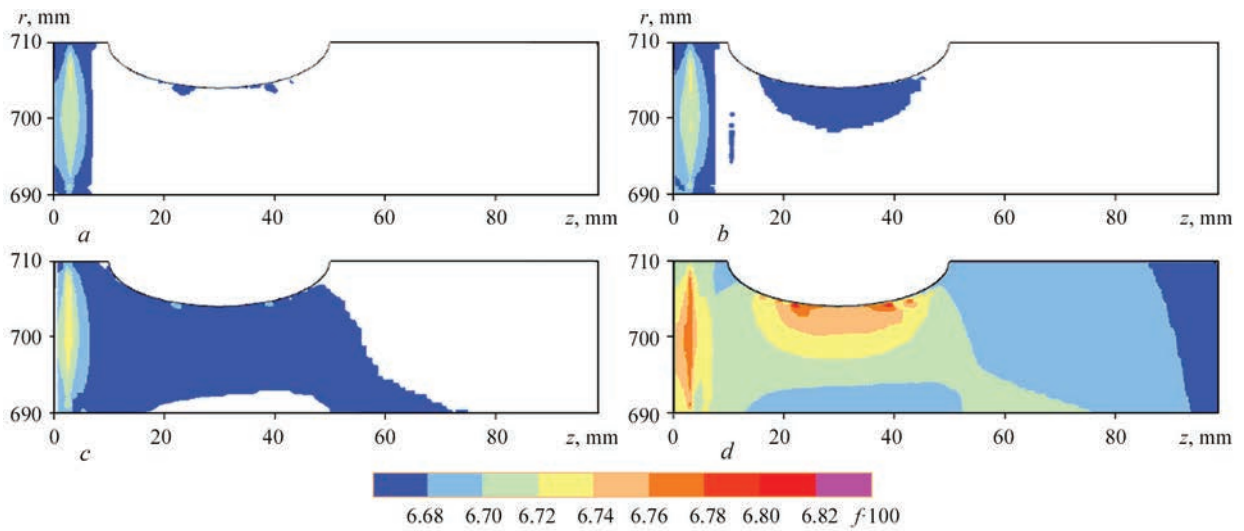


Figure 7. Distribution of the field of volume concentration f of ductile fracture pores in the cross-section of pipeline element ($D \times t = 1420 \times 20$ mm, X65) with local metal loss at the periphery of a circular weld at different values of external pressure P : *a* — 16.5 MPa; *b* — 17.0; *c* — 20.0

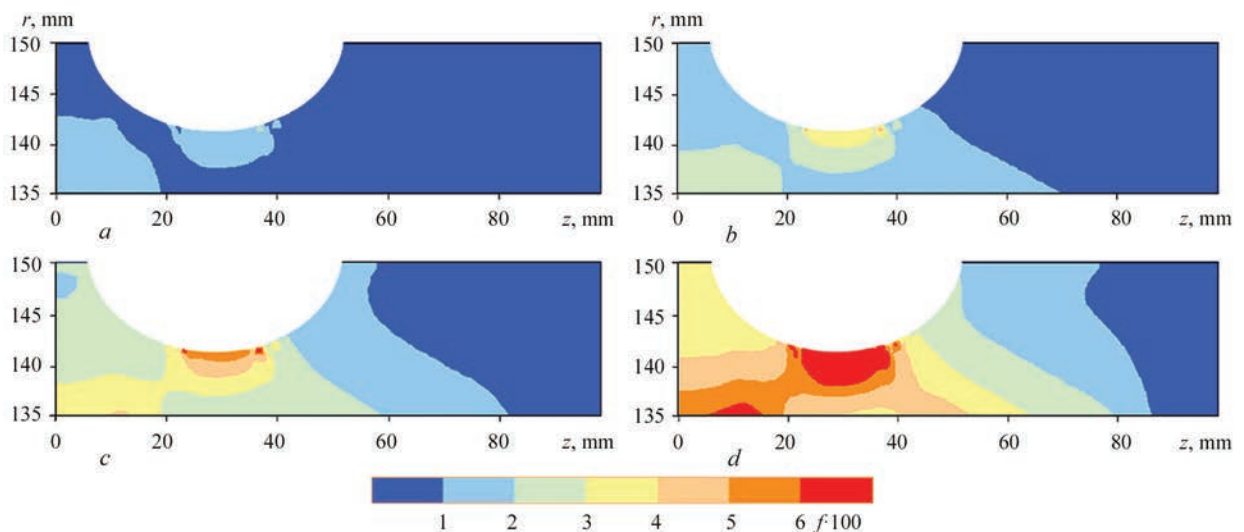


Figure 8. Distribution of the field of volume concentration f of ductile fracture pores in the cross-section of pipeline element wall ($D \times t = 300 \times 15$ mm, 10GN2MFA) with local metal loss at the periphery of a circular weld at different time τ of high-temperature operation ($T = 650$ °C, $P = 13$ MPa): *a* — 400 s; *b* — 800 s; *c* — 1200 s; *d* — 1500 s

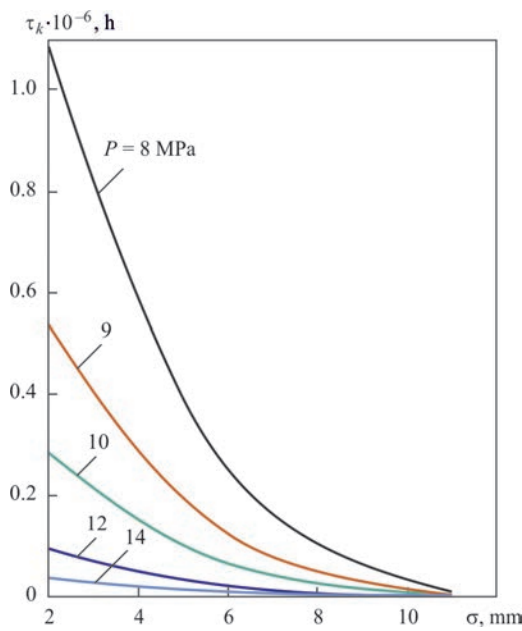


Figure 9. Dependencies of time to macroscopic fracture of pipeline element τ_k ($D \times t = 300 \times 15$ mm, 10GN2MFA) on the depth of thinning defect δ in the area of an assembly weld at different values of internal pressure P (defect length $2s = 30$ mm)

geometrical anomaly has a fundamentally different impact on PE state. So, in the case of an element of process pipeline from 10GN2MFA steel ($D \times t = 300 \times 15$ mm) with semi-elliptical local wall thinning ($2s \times 2u \times \delta = 40 \times 40 \times 7$ mm) on the pipe outer surface it was shown that the defect presence causes similar regularities of subcritical damage accumulation in high-temperature operation ($T = 625$ °C, $P = 13$ MPa). However, the main deformation mechanism here is high-temperature creep (Figure 8). So, at the start of operation the spatial distribution of concentration of ductile fracture pores is characterized by two local maximums, namely near the defects and in the weld area. Further development of creep deformations causes an increase and combining of these two areas of subcritical damage, that determines the limit

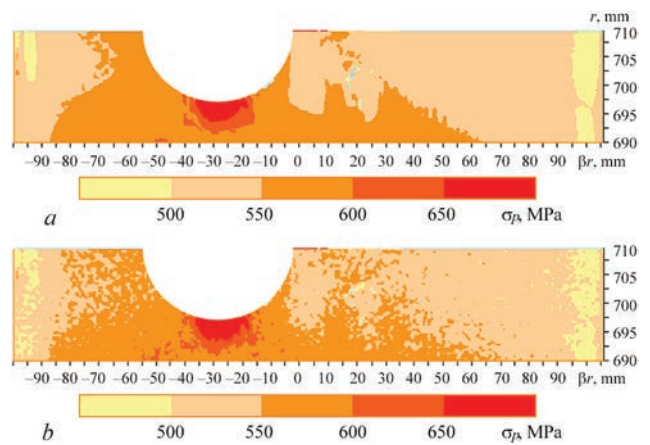


Figure 11. Distribution of residual equivalent stresses in a pipeline ($D \times t = 1420 \times 20$ mm, X65 steel) with external corrosion defect ($2s \times 2u \times \delta = 55 \times 40 \times 10$ mm) at limit external pressure: *a* — traditional calculation with constant material properties; *b* — computation by Monte-Carlo algorithm

state of the welded pipeline. It should be noted that a characteristic feature of PE fracture during material creep is relaxation of post-welding stresses, as a result of accumulation of irreversible creep deformations that gradually lowers the growth rate of ductile fracture pores in the weld area.

Assessment of admissibility of a defect of local thinning of pipeline wall for the case of low-temperature operation differs essentially from the one which concerns the conditions of force impact at high temperatures: corrosion-erosion defect, which at analysis of static strength belongs to admissible ones and slightly lowers PE load-carrying capacity in a certain range of internal pressure values, during the operation period leads to damage accumulation and further macroscopic fracture of the structure that should be taken into account at substantiation of the residual service life of critical PE. Effect of the dimensions of the defect of local thinning of pipeline wall for the period up to macroscopic fracture of pipeline element, τ_k , that was studied by numerical modeling in the case

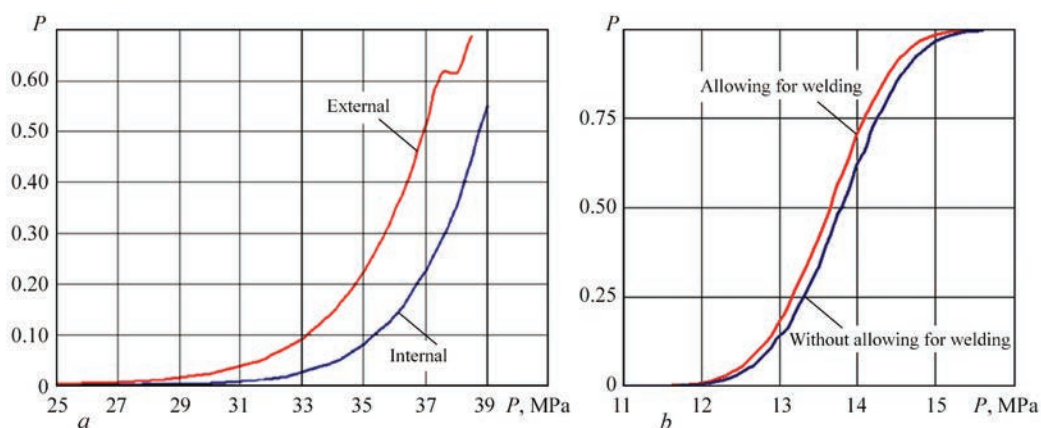


Figure 10. Effect of the surface of thinning defect location ($2s \times 2u \times \delta = 100 \times 80 \times 9$ mm, $D \times t = 530 \times 18$ mm, X65) — (*a*) and presence of a circular weld ($2s \times 2u \times \delta = 50 \times 50 \times 5$ mm, $D \times t = 530 \times 10$ mm, AMg6) — (*b*) on PE fracture probability p at different values of internal pressure P

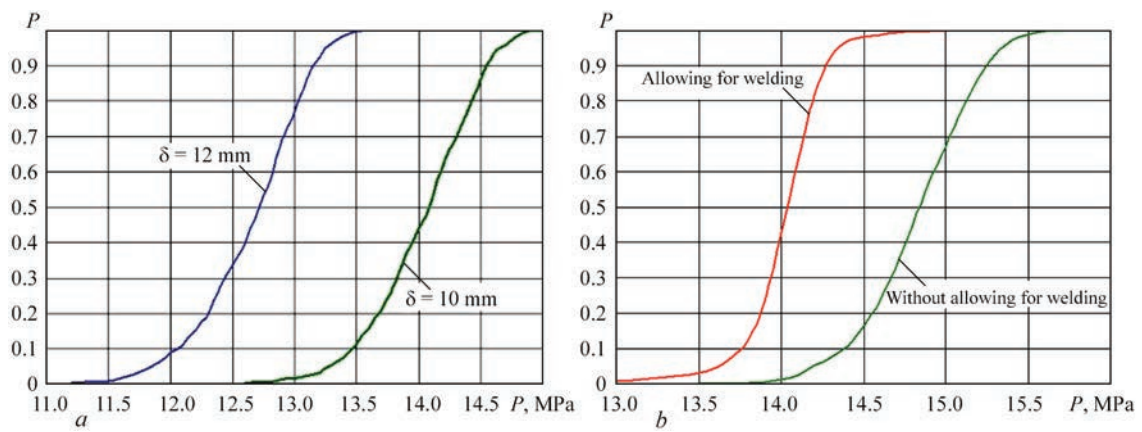


Figure 12. Dependencies of pipeline fracture probability p ($D \times t = 1420 \times 20$ mm, X65) with external corrosion defect ($2s \times 2u \times \delta = 20 \times 20 \times 10$ mm) on internal pressure P , taking into account stochastic nonuniformity of properties: a — for different values of defect depth δ ; b — taking into account the presence of a weld at the defect periphery

of PE with defects of different depth δ ($T = 650$ °C, $P = 13$ MPa), is of a pronounced non-linear nature (Figure 9). This is related to multifactoriality of the processes of elasto-plastic deformation and fracture of a pipeline with certain residual post-welding SSS.

Results of finite-element computation of SSS of a pipeline with the detected corrosion-erosion defects enable numerical prediction of PE fracture probability within the Weibull theory (8)–(9). Here, not only spatial distribution of the fields of stresses (strains), interaction of the fields of stresses of the first and second kind, but also actual characteristics of ductile fracture resistance of the material are taken into account. So, application of 3D models of the stress-strain and damage states of PE with a 3D defect of local wall thinning allow with minimum conservatism taking into account the features of actual geometry of the structure, in particular, defect location surface (Figure 10, a). Moreover, it is thus possible to perform quantitative analysis of the impact of assembly welding at different stages of loading by internal pressure right up to the limit state (Figure 10, b).

For numerical analysis of the impact of stochastic nature of distribution of the properties of the studied defective PE material on the current SSS and limit state, it was assumed that the spatial scatter is demonstrated by the material yield limit (by the normal law, $\alpha = 408$ MPa, $\beta = 10.34$ MPa), critical deformation of initiation of ductile fracture pores (by Weibull distribution, $A_e = 0.001$, $B_e = 0.0061$, $\eta_e = 4$), initial concentration of ductile fracture pores (by Weibull distribution, $A_f = 0.0001$, $B_f = 0.000397$, $\eta_f = 2$). Presence of a defect in the area of a circular assembly weld under the conditions of operational loading by internal pressure only slightly affects the nature of the change of current and limit SSS, because of scatter of PE material properties (Figure 11).

Thus, we can conclude that despite the nonuniform properties of the material, the nature of interaction of residual stresses in the welding area and of operational stresses (taking into account the geometrical stress raiser) remains the same, as in traditional modeling, within the models of a uniform continuous medium. The nonuniformity the most significantly affects the macrofracture initiation and onset of the limit state of the structure: appearance of weaker regions in atypical zones leads to lower breaking pressure, or, contrarily, to strengthening of the weakest regions, and strengthens the load-carrying capacity of the structure.

Application of direct Monte-Carlo methods, alongside the respective finite-element solution of multi-physical problems of limit state determination, allows evaluation of the impact of typical parameters of the actual state of pipeline defective sections on their reliability, taking into account the indeterminateness of spatial distribution of structure material properties. In particular, it is known that defect depth has the greatest impact on the load-carrying capacity of PE with a defect of local corrosion-erosion thinning. For the above case of PE with a detected thinning defect, the fracture probability, depending on internal pressure at different values of defect depth, is shown in Figure 12, a . Increase of defect depth causes a shifting of $p(P)$ curve at preservation of similarity. It is explained by that this range of variation of the radial defect size does not cause a change in the fracture mechanism.

Presence of a defect in the area of assembly weld has an additional negative effect on the load-carrying capacity of the pipeline defective area that is due to intensification of the growth of ductile fracture pores in the areas of higher stiffness of the stressed state. This is quantitatively described by the respective probabilistic curves, the example of which is given in Figure 12, b . From these data one can see that the weld presence changes the susceptibility of a defective PE

to fracture under the impact of internal pressure: in addition to the anticipated shifting of $p(P)$ curve relative to the case of an unwelded pipe, the slope of the probabilistic fracture curve decreases in the presence of the weld.

Conclusions

1. A set of mathematical models was developed for prediction of simultaneous processes of thermal deformation and subcritical fracture of metal of welded elements of the main and technological pipelines and pressure vessels with detected defects of local corrosion-erosion metal loss under the conditions of welding and further operation. A satisfactory accuracy of numerical determination of limit pressure in PE with surface defects is shown.

2. Based on the results of numerical studies of limit state of typical pipeline elements with surface metal losses near the areas of assembly or repair welding it is shown that the interaction of these two anomalies of the structure consists in formation of a common area of subcritical fracture by the ductile mechanism, which is the zone of potential formation of a macroscopic defect and violation of pipe integrity. For the case of high-temperature operation of pipelines this effect is more significant, due to additional deformation of metal by the creep mechanism.

3. Procedures were developed for numerical determination of fracture probability of welded pipeline elements with detected surface defects of local corrosion-erosion loss of metal based on the statistical Weibull theory of strength and direct Monte-Carlo method. As regards pipe steels of different strength classes, as well as aluminium alloys, values of Weibull coefficients as a function of material properties, were derived.

4. By the results of numerical studies of the impact of spatial nonuniformity of PE properties on fracture probability it is shown that, despite the nonuniformity of material properties the nature of interaction of residual stresses in the welding area and operating stresses (taking into account the geometrical stress raiser) remains the same as at traditional modeling within the models of uniform continuous medium.

1. Lemaitre, J., Desmorat, R. (2005) *Engineering damage mechanics. Ductile, Creep, Fatigue and Brittle Failures*. Berlin, Springer-Verlag. <https://doi.org/10.1007/b138882>.
2. de Geus, T.W.J., Peerlings, R.H.J., Geers, M.G.D. (2015) Microstructural modeling of ductile fracture initiation in multi-

- phase materials. *Engineering Fracture Mechanics*, **147**, 318–330. <https://doi.org/10.1016/j.engfracmech.2015.04.010>.
3. Makhnenko, V.I. (2013) Problems of examination of modern critical welded structures. *The Paton Welding J.*, **5**, 21–28.
4. Wei, Y., Zhang, L., Au, F.T.K. et al. (2016) Thermal creep and relaxation of prestressing steel. *Construction and Building Materials*, **128**, 118–127. <https://doi.org/10.1016/j.conbuildmat.2016.10.068>.
5. Velikoivanenko, E., Milenin, A., Popov, A. et al. (2019) Methods of numerical forecasting of the working performance of welded structures on computers of hybrid architecture. *Cybernetics and Systems Analysis*, **55**(1), 117–127. <https://doi.org/10.1007/s10559-019-00117-8>.
6. Xue, L. (2007) Damage accumulation and fracture initiation in uncracked ductile solids subject to triaxial loading. *Int. J. of Solids and Structures*, **44**, 5163–5181. <https://doi.org/10.1016/j.ijsolstr.2006.12.026>.
7. Milenin, A.S., Velikoivanenko, E.A., Rozyuka, G.F., Pivtorak, N.I. (2016) Simulation of subcritical damage of metal in welded pipeline elements at low-cycle loading. *Tekhn. Diagnost. i Nerazrush. Kontrol*, **4**, 14–20. <https://doi.org/10.15407/tdnk2016.04.03>.
8. Jones, N. (2012) *Structural Impact*. Second edition. Cambridge University Press. <https://doi.org/10.1017/CBO9780511624285>
9. Lemaitre, J., Chaboche, J.-L. (1990) *Mechanics of Solid Materials*. Cambridge University Press. <https://doi.org/10.1017/CBO9781139167970>.
10. Milenin, A.S., Velikoivanenko, E.A., Rozyuka, G.F., Pivtorak, N.I. (2013) Simulation of processes of initiation and propagation of ductile fracture pores in welded structures. *The Paton Welding J.*, **9**, 26–31.
11. Chen, Z., Butcher, C. (2013) *Micromechanics Modeling of Ductile Fracture*. Springer Netherlands. <https://doi.org/10.1007/978-94-007-6098-1>.
12. Milenin, O. (2017) Numerical prediction of the current and limiting states of pipelines with detected flaws of corrosion wall thinning. *J. of Hydrocarbon Power Engineering*, **4**(1), 26–37.
13. Lindquist, E.S. (1994) Strength of materials and the Weibull distribution. *Probabilistic Engineering Mechanics*, **9**(3), 191–194. [https://doi.org/10.1016/0266-8920\(94\)90004-3](https://doi.org/10.1016/0266-8920(94)90004-3).
14. Milenin, A., Velikoivanenko, E., Rozyuka, G., Pivtorak, N. (2019) Probabilistic procedure for numerical assessment of corroded pipeline strength and operability. *Int. J. of Pressure Vessels and Piping*, **171**, 60–68. <https://doi.org/10.1016/j.ijpvp.2019.02.003>.
15. Makhnenko, V.I. (2016) *Safe operating life of welded joints and assemblies of modern structures*. Kiev, Naukova Dumka [in Russian].
16. Lawless, J.F. (2002) *Statistical Models and Methods for Lifetime Data*. John Wiley & Sons, Inc., Hoboken, New Jersey. <https://doi.org/10.1002/9781118033005>.
17. Cronin, D. (2000) *Assessment of Corrosion Defects in Pipelines*. PhD thesis. University of Waterloo.
18. Kitching, R., Zarrabi, K. (1982) Limit and burst pressures for cylindrical shells with part-through slots. *Int. J. of Pressure Vessels and Piping*, **10**(4), 235–270. [https://doi.org/10.1016/0308-0161\(82\)90035-7](https://doi.org/10.1016/0308-0161(82)90035-7)

Received 19.08.2020